INTERNATIONAL JOURNAL OF
NUMERICAL ANALYSIS AND MODELING
Volume 22, Number 4, Pages 534–555

doi: 10.4208/ijnam2025-1023

SCHWARZ METHOD IN A GEOMETRICAL MULTI-SCALE DOMAIN WITH CONTINUOUS OR DISCONTINUOUS JUNCTIONS

MARIE-CLAUDE VIALLON

Abstract. A model parabolic linear partial differential equation in a geometrical multi-scale domain is studied. The domain consists of a two-dimensional central node, and several one-dimensional outgoing branches. The physical coupling conditions between the node and the branches are either continuity of the solution or continuity of the normal flux. An iterative Schwarz method based on Robin transmission conditions is adjusted to the problem in each case and formulated in substructured form. The convergence of the method is stated. Numerical results when the method is used as preconditioner for a Krylov method (GMRES) are provided.

Key words. Finite volume scheme, parabolic problem, multi-scale domain, domain decomposition, stability and convergence of numerical methods, Schwarz methods, Robin interface condition.

1. Introduction

Geometrical multi-scale problems involve coupling dimensionally-heterogeneous partial differential equations. These are generally reduced models of reality for which computational costs are much lower, although the full-dimensional models have to be kept in the neighborhoods of the bifurcations or junctions. Such dimensionally-heterogeneous problems have been studied in different fields. In some problems of this type, such as fluid flow in a fracture in a porous medium, or blood flow in a small vessel in biological tissue, the part of the domain whose geometric dimension is reduced is included in a part of the domain whose original dimension is retained [30, 15]. In this paper, we place ourselves in a context where parts of the domain of different dimensions are side by side. In [28, 29], where domains of different geometric dimensions are juxtaposed, domain decomposition methods such that the interfaces take place at the frontier between the domains of different dimensionalities are used. The partitioning methodology takes full advantage of the small number of interface unknowns (which is not the case with an embedded model). In [3], a general theoretical framework, which generalizes this methodology, is developed by recasting the variational formulation in terms of coupling interface variables. The last papers [3, 28, 29] present examples in the fields of heat transfer, linear elasticity, hydraulic networks.

Here, we consider a model problem posed in a domain which derives from a network of rods. The rod structures are some connected unions of cylinders. They are for instance systems of pipes in industrial installations or canal systems. Often, rods are considered as one-dimensional (1D) at some distance from the junctions. This is particularly true for modeling the human blood circulatory system [5, 37].

Continuing a study whose results are presented in [33, 34, 35, 36, 41], we consider here the heat equation set in a geometrical multi-scale domain called D_ε that derives from a two-dimensional (2D) thin rod structure Ω_ε. This rod structure itself derives from a very simple graph that is a single bundle with one node O from which p

Received by the editors on May 30, 2024 and, accepted on January 14, 2025.
2000 *Mathematics Subject Classification.* 35K05, 65F10, 65N08, 65N12, 65N55.

edges, $e_j = [O, O_j], j = 1, ..., p$, depart. The length of the edge $|e_j| = l_j, j = 1, ..., p$. The axis Ox^{e_j} has the direction of $[OO_j)$ and a local Cartesian coordinate systems $(O, x^{e_j}, y^{e_j}), j = 1, ..., p$, is considered. The thin rod structure is an union of p thin rectangles to which a bounded domain ω_0^ε is added at the center to smooth out the corners. Each rectangle being carried by a single edge, the rectangle on edge e_j is defined by $\{(x^{e_j}, y^{e_j}) \in I\!R^2 : x^{e_j} \in (0, l_j), y^{e_j} \in (-\theta_j\varepsilon/2, \theta_j\varepsilon/2)\}, j = 1, ..., p$, where $\varepsilon > 0$ is a small parameter and $\theta_j, j = 1, ..., p$, are positive numbers independent of ε. We build D_ε from Ω_ε, keeping a small 2D area around the node as it is, which we call $\Omega(0)$, and assuming that each rectangular branch from this area is now reduced to the 1D central edge around which it is built. To be more precise, let $\delta > 0$, $\Omega(0)$ is the truncated at the distance δ from the junction part of Ω_ε containing the junction. Ω_ε and D_ε can be seen from Figure 1.

The segments $\gamma_j, j = 1, ..., p$, are the 1D-2D interfaces at $x^{e_j} = \delta$ in D_ε and from the above $|\gamma_j| = \theta_j\varepsilon$. The part of the jth rectangular branch that is reduced to dimension 1 in space is denoted S_j. Even if the dependence of δ versus ε is not the subject of this paper, remember that if δ is of order $\varepsilon|ln(\varepsilon)|$ and if the source term is assumed to only depend on the longitudinal variables, then it was proved by asymptotic analysis that the solutions of the heat equation on D_ε and Ω_ε are very close to each other (for more details see Theorem 6.2 in [35] and Theorem 3.3 in [36]). This justifies to work in D_ε.

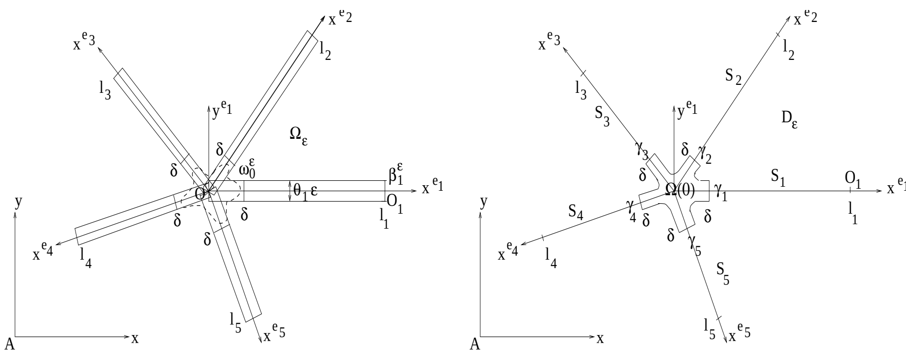

FIGURE 1. The rod structure Ω_ε on the left and the geometrical multi-scale domain D_ε on the right.

Two options are provided for the 1D-2D physical coupling conditions on the interfaces $\gamma_j, j = 1, ..., p$: the solution and the mean value of the flux are continuous, or the flux and the mean value of the solution are continuous. First, monolithic finite volume numerical scheme of hybrid dimension was defined in [35] and [41] in either case. These schemes lead to linear systems that give the volume solution of the model problem and they are solved by a direct method. Second, iterative substructuring domain decomposition methods used as preconditioner for a Krylov method (GMRES, see [40]) and such that the interfaces take place at γ_j were also used. They result in an interface system at each time step, which depends on the 1D and 2D separated problems (we are not here in the waveform relaxation setting described in [24]). However, the boundary conditions chosen to define the 2D separated problem were mainly pointwise Dirichlet conditions when the solution is continuous, or pointwise Neumann conditions when the flux is continuous.

The aim of this paper is to generalize and study a discrete version of P. L. Lions' algorithm (see [31]), which is an adaptation of the classical parallel Schwarz algorithm (see [17, 21] and the references in it), for solving our linear model problem in D_ε. The P. L. Lions' algorithm improves on the classical Schwarz method by replacing Dirichlet transmission conditions between subdomains with Robin transmission conditions. Then it is convergent whether or not there is overlap between subdomains, whereas the classical method does not converge without overlap. We are investigating this method, which works with non-overlapping subdomains, as it seems particularly well suited to the heterogeneity of D_ε. Our work is focused on a discrete version of this Schwarz method based on Robin transmission conditions. More precisely, we study it in substructured form. As mentioned above, the substructured form is especially appropriate because the number of interface unknowns is typically small and calculation costs are low. In [11, 12], the authors consider, for general elliptic problems, a substructured version of the classical overlapping Schwarz method with several subdomains and crosspoints. The authors propose a correction to improve convergence as the number of subdomains increases, and analyse the two-level methods obtained. In [11], spectral coarse spaces are considered with coarse space functions defined exclusively on the interfaces. In [12], two-level and multilevel Schwarz methods defined on the substructures are considered, for which the coarse correction is performed on coarser interface grids. We do not consider two-level methods here. In our opinion, the question of scalability is not relevant in the present context, where the number of subdomains of different dimensions is given at the start, and where only the coupling between subdomains of different dimensions is dealt with. The generalization of the Schwarz method from subdomains of the same dimension to subdomains of different dimensions requires specific Robin boundary conditions at the interfaces for the 2D separated problem since the problem is not well-defined with pointwise Robin relations. As the performance of the classical Schwarz method depends strongly on the size of the overlap, a new class of optimized Schwarz algorithms were developed and used even more general boundary conditions than Robin ones. It was first suggested in [25] to use nonlocal transmission conditions to lead to optimal results in terms of iteration counts in domain decomposition. Numerous approximations of these conditions were developed for different problems by many authors (see for instance [2, 13, 14, 16, 18, 19, 20, 23, 26, 27, 32, 39]). Nevertheless, the iterative Schwarz method is used in our work in substructured form. This gives interface systems with a very few number of unknowns (one or two per interface). Moreover, the method is used as preconditioner for GMRES. Consequently, the number of iterations needed to achieve convergence by using GMRES is already very low and there is no need to optimize the transmission conditions.

Regarding the discrete version of the Schwarz method, several discretizations were studied in [1, 6, 22], and [8] where a finite volume scheme for convection diffusion equation on non matching grids is proposed and studied. In this paper we provide a finite volume discretization of the method adapted to our hybrid dimension transmission conditions. Then we obtain theoretical convergence results. We compare the two physical transmission conditions (with or without continuity) by observing how the method, in substructured form and accelerated by GMRES, behaves in numerical terms.

This work is organized as follows. Section 2 presents the substructured form of the iterative Schwarz method to solve the model problem on the one hand with physical transmission conditions that ensure the continuity of the solution, on the other hand with physical transmission conditions that ensure only a weak continuity on average of the solution. In Section 3, convergence of the method is proved in both cases. In Section 4, numerical results are given.

2. The Schwarz scheme

2.1. The hybrid dimension problem and the discretization. A description of all the notations used in this paper can be found in [41].

The boundary value problem in the domain D_ε is the following:

$$
(1) \qquad \begin{cases} \dfrac{\partial v_j}{\partial t}(x^{e_j},t) - \dfrac{\partial^2 v_j}{\partial x^{e_j 2}}(x^{e_j},t) = f_j(x^{e_j},t),\ x^{e_j} \in (\delta, l_j), t \in (0,T), \\ j = 1,...,p, \\ v_j(x^{e_j},0) = 0,\ x^{e_j} \in (\delta, l_j), j = 1,...,p, \\ v_j(l_j,t) = 0, t \in (0,T), j = 1,...,p, \\ \dfrac{\partial u}{\partial t}(x,y,t) - \triangle u(x,y,t) = f(x,y,t),\ (x,y) \in \Omega(0), t \in (0,T), \\ u(x,y,0) = 0,\ (x,y) \in \Omega(0), \\ \dfrac{\partial u}{\partial n}(x,y,t) = 0,\ (x,y) \in \partial\Omega(0) \backslash (\cup_{j=1}^{p} \gamma_j), t \in (0,T), \end{cases}
$$

supplemented by the transmission conditions

$$
(2) \qquad u(x,y,t) = v_j(\delta,t),\ (x,y) \in \gamma_j, j = 1,...,p, t \in (0,T),
$$

$$
(3) \qquad \frac{1}{|\gamma_j|}\int_{\gamma_j} \frac{\partial u}{\partial n}(\cdot,t)d\gamma = \frac{\partial v_j}{\partial x^{e_j}}(\delta,t), j = 1,...,p, t \in (0,T),
$$

which are the first option, or by these ones

$$
(4) \qquad \frac{1}{|\gamma_j|}\int_{\gamma_j} u(\cdot,t)d\gamma = v_j(\delta,t), j = 1,...,p, t \in (0,T),
$$

$$
(5) \qquad \frac{\partial u}{\partial n}(x,y,t) = \frac{\partial v_j}{\partial x^{e_j}}(\delta,t), (x,y) \in \gamma_j, j = 1,...,p, t \in (0,T),
$$

which are the second option.

We assumed in [41] that the functions f_j (respectively f) were smooth and independent of ε, were constant with respect to (x,y) in some neighborhood of $O_j, j = 1,...,p$ (respectively O), and vanished for $t \leq t_0, t_0 > 0$. In addition, we assumed they are such that the partial derivatives of u in $\overline{\Omega(0)}$ and v_j in $[\delta, l_j], j = 1,...,p$, exist and are continuous till the order two. This enabled us to obtain error estimates.

The problem (1-2-3) is referred to as (1)"csa", with pointwise continuity of the solution and continuity in average of the flux over the junctions, and the problem (1-4-5) is referred to as (1)"dsa", with continuity in average of the solution (the solution may be discontinuous), and continuity of the flux. Note that these are simply multidomain formulations of the heat equation set in $\Omega_\varepsilon \times [0,T]$. The subdomains are the 1D branches $S_j, j = 1,...,p$, and the 2D domain $\Omega(0)$. They do not overlap. The interfaces are the segments $\gamma_j, j = 1,...,p$. The following study could be done in the same way in a more general domain such as a thin rod structure with several nodes as described in [33].

Space and time meshing is the same for both options. The discretization was carried out in [35] section 7 and [41] section 2. The main points are summarized here.

Let us define the mesh of each 1D branch S_j on the axis Ox^{e_j}, $j = 1, ..., p$: we choose $N_j \in I\!N^*$, and $N_j + 1$ distinct and increasing values $x^{e_j}_{i+1/2}, i = 0, ..., N_j$, such that $x^{e_j}_{1/2} = \delta, x^{e_j}_{N_j+1/2} = l_j$. Denote $h^{e_j}_i = x^{e_j}_{i+1/2} - x^{e_j}_{i-1/2}, i = 1, \ldots, N_j$. Then we choose N_j points $x^{e_j}_i, i = 1, ..., N_j$, such that $x^{e_j}_{i-1/2} \leq x^{e_j}_i \leq x^{e_j}_{i+1/2}$. Set $x^{e_j}_0 = \delta, x^{e_j}_{N_j+1} = l_j$, and $h^{e_j}_{i+1/2} = x^{e_j}_{i+1} - x^{e_j}_i, i = 0, ..., N_j$.

Now let us define the mesh over $\Omega(0)$. It consists of a set $\mathcal{T}$ of open polygonal convex subsets K called control volumes, a family $\mathcal{E}$ of edges σ of the control volumes, and a family $\mathcal{P}$ of points x_K in each control volume K. The set of the interior edges is named $\mathcal{E}_{int}$, and for any $K \in \mathcal{T}$, $\mathcal{E}_K$ is the set of edges in ∂K. The mesh $\mathcal{T}$ is assumed to be admissible that is:

– For any $(K, L) \in \mathcal{T}^2, K \neq L,$ one of three following assertions holds: either $\overline{K} \cap \overline{L} = \emptyset,$ or $\overline{K} \cap \overline{L}$ is a common vertex of K and L, or $\overline{K} \cap \overline{L} = \overline{\sigma}, \sigma$ being a common edge of K and L denoted by $\sigma_{K/L}$.

and

– The family $\mathcal{P} = (x_K)_{K \in \mathcal{T}}$ is such that for any $K \in \mathcal{T}, x_K \in \overline{K}$. For any $(K, L) \in \mathcal{T}^2, K \neq L,$ it is assumed that $x_K \neq x_L$ and that the straight line going through x_K and x_L is orthogonal to $\sigma_{K/L}$.

– For any $K \in \mathcal{T},$ if $\sigma \in \mathcal{E}_K$ and $\sigma \subset \partial\Omega(0),$ it is assumed that $x_K \notin \sigma$, and that the orthogonal projection of x_K on the straight line containing the edge $\sigma,$ belongs to σ.

Thanks to these last items, it is easy to obtain a consistent approximation of the normal derivative along each edge $\sigma_{K/L} \in \mathcal{E}_{int}$ (since the direction of the vector defined by the two points x_K and x_L is the same as that of the normal to the edge $\sigma_{K/L}$ separating the control volumes K and L), and each edge on the boundary.

Let d_σ be the distance between x_K and x_L if $\sigma = \sigma_{K/L}$, or the distance between x_K and σ if $\sigma \in \mathcal{E}_K$ and $\sigma \subset \partial\Omega(0)$.

For any $K \in \mathcal{T}$, let $m(K)$ be the area of K. For any $\sigma \in \mathcal{E}$, let $m(\sigma)$ be the length of σ.

The time step is $\Delta t \in (0, T)$, $N_{\Delta t} = \max\{n \in I\!N, n\,\Delta t < T\}$. Let $t_n = n\,\Delta t$, for $n \in \{0, ..., N_{\Delta t} + 1\}$.

The value $v^n_{j,i}$ is an approximation of $v_j(x^{e_j}_i, t_n), i = 0, ..., N_j + 1, j = 1, ..., p$, and the value u^n_K is an approximation of $u(x_K, t_n), K \in \mathcal{T}, n \in \{0, ..., N_{\Delta t} + 1\}$. The values $v^n_{j,i}, i = 1, ..., N_j$, and u^n_K are unknowns of the monolithic schemes (schemes that give the volume solution by a direct method). The iterative Schwarz method requires the introduction of additional unknowns that are Robin quantities to the left and right of each interface. The construction of the iterative Schwarz method is shown below, first for (1)"csa", then for (1)"dsa".

2.2. Continuity of the solution and continuity in average of the normal flux. Here, we consider the first option, i.e. (1)"csa". Then the values of the solution on the right and on the left of the interface γ_j at time t_n are coincident due to the transmission conditions (2). Their approximations in the monolithic scheme previously established in [35] are both denoted by $v^n_{j,0}$. Let us start by recalling the monolithic scheme. Remember that the numerical approximation of the fluxes in $(1)_4$ and (3) is simply done by finite difference due to the orthogonality condition of the mesh $\mathcal{T}$. The monolithic scheme is:

$$(6)\quad \begin{cases} h_i^{e_j}\dfrac{v_{j,i}^{n+1}-v_{j,i}^{n}}{\Delta t}+F_{i+1/2}^{j,n+1}-F_{i-1/2}^{j,n+1}=h_i^{e_j}f_i^{e_j,n},\ i=1,...,N_j, j=1,...,p,\\ F_{i+1/2}^{j,n+1}=-\dfrac{v_{j,i+1}^{n+1}-v_{j,i}^{n+1}}{h_{i+1/2}^{e_j}},\ i=1,\dots,N_j,\ v_{j,N_j+1}^{n+1}=0, j=1,...,p,\\ f_i^{e_j,n}=\dfrac{1}{h_i^{e_j}}\displaystyle\int_{x_{i-1/2}^{e_j}}^{x_{i+1/2}^{e_j}} f_j(x_1,t_{n+1})dx_1,\ i=1,\dots,N_j, j=1,...,p, \end{cases}$$

$$(7)\quad F_{1/2}^{j,n+1}=-\frac{v_{j,1}^{n+1}-v_{j,0}^{n+1}}{h_{1/2}^{e_j}}, j=1,...,p,$$

$$(8)\quad \begin{cases} m(K)\dfrac{u_K^{n+1}-u_K^{n}}{\Delta t}+\displaystyle\sum_{\sigma\in\mathcal{E}_K}F_{K,\sigma}^{n+1}=m(K)f_K^n,\ \forall K\in\mathcal{T},\\ F_{K,\sigma}^{n+1}=-\dfrac{m(\sigma)}{d_\sigma}(u_L^{n+1}-u_K^{n+1}),\ \forall\sigma\in\mathcal{E}_{int}\ ,\ \text{if } \sigma=\sigma_{K/L},\\ F_{K,\sigma}^{n+1}=0,\forall\sigma\subset\partial\Omega(0)\backslash(\cup_{j=1}^{p}\gamma_j),\\ f_K^n=\dfrac{1}{m(K)}\displaystyle\int_K f(x,t_{n+1})dx,\ \forall K\in\mathcal{T}, \end{cases}$$

$$(9)\quad F_{K,\sigma}^{n+1}=-\frac{m(\sigma)}{d_\sigma}(v_{j,0}^{n+1}-u_K^{n+1}),\forall\sigma\subset\gamma_j\ ,\ \sigma\in\mathcal{E}_K, j=1,...,p,$$

$$(10)\quad \frac{v_{j,1}^{n+1}-v_{j,0}^{n+1}}{h_{1/2}^{e_j}}=\frac{1}{|\gamma_j|}\sum_{\sigma\subset\gamma_j,\sigma\in\mathcal{E}_K}\frac{m(\sigma)}{d_\sigma}(v_{j,0}^{n+1}-u_K^{n+1}), j=1,...,p,$$

with the initial condition

$$\begin{cases} u_K^0=0,\forall K\in\mathcal{T},\\ v_{j,i}^0=0, i=1,...,N_j, j=1,...,p. \end{cases}$$

Relation $(6)_1$ is the discretization of $(1)_1$, and the numerical flux $F_{i+1/2}^{j,n+1}$ in $(6)_2$ and (7) when $i=0$ is the discretization of $-\dfrac{\partial v_j}{\partial x^{e_j}}(x_{i+1/2}^{e_j},t_{n+1})$. Relation $(8)_1$ is the discretization of $(1)_4$, the numerical flux $F_{K,\sigma}^{n+1}$ in $(8)_2$ and (9) is the discretization of $-\displaystyle\int_\sigma \frac{\partial u}{\partial n}(\cdot,t_{n+1})d\gamma$ when $\sigma\in\mathcal{E}_K$. Relation (10) is the discretization of (3).

Then let us write an equivalent version of this scheme where new variables needed to define the Schwarz method are introduced. Let us keep $v_{j,0}^n$ as the approximation of the solution on the S_j side of γ_j and let us use a new unknown $u_{\gamma,j}^n$, approximation of the solution on the $\Omega(0)$ side of γ_j, to write a slightly different equivalent version of the monolithic scheme, in which fluxes at the interfaces on the $\Omega(0)$ side, originally defined by (9), are now expressed in terms of these new variables:

$$(11)\quad F_{K,\sigma}^{n+1}=-\frac{m(\sigma)}{d_\sigma}(u_{\gamma,j}^{n+1}-u_K^{n+1}),\forall\sigma\subset\gamma_j\ ,\ \sigma\in\mathcal{E}_K, j=1,...,p.$$

The discretization of (2) and (3) becomes

$$(12)\quad \begin{cases} u_{\gamma,j}^{n+1}=v_{j,0}^{n+1}, j=1,...,p,\\ \dfrac{v_{j,1}^{n+1}-v_{j,0}^{n+1}}{h_{1/2}^{e_j}}=\dfrac{1}{|\gamma_j|}\displaystyle\sum_{\sigma\subset\gamma_j,\sigma\in\mathcal{E}_K}\dfrac{m(\sigma)}{d_\sigma}(u_{\gamma,j}^{n+1}-u_K^{n+1}), j=1,...,p. \end{cases}$$

We are now able to define a version of the Schwarz method specifically adapted to our problem using a simple change of unknowns in (6-7-8-11-12). New unknowns are Robin quantities, which depend on $v^n_{j,0}$ and $u^n_{\gamma,j}$, defined below. First, the iterative Schwarz method (defined in volume) is derived from the above, followed by the iterative substructured version.

For $j = 1, ..., p$, let $q_j \neq 0$, and let us define the quantities:

$$(13)\qquad \begin{cases} r^{n+1}_j = \dfrac{v^{n+1}_{j,1} - v^{n+1}_{j,0}}{h^{e_j}_{1/2}} + q_j v^{n+1}_{j,0}, \text{ and } r^{n+1}_{-j} = -\dfrac{v^{n+1}_{j,1} - v^{n+1}_{j,0}}{h^{e_j}_{1/2}} + q_j v^{n+1}_{j,0}, \\ r^{n+1}_{0j} = \frac{1}{|\gamma_j|}\sum_{\sigma\subset\gamma_j,\sigma\in\mathcal{E}_K} \frac{m(\sigma)}{d_\sigma}(u^{n+1}_{\gamma,j} - u^{n+1}_K) + q_j u^{n+1}_{\gamma,j}, \\ r^{n+1}_{-0j} = -\frac{1}{|\gamma_j|}\sum_{\sigma\subset\gamma_j,\sigma\in\mathcal{E}_K} \frac{m(\sigma)}{d_\sigma}(u^{n+1}_{\gamma,j} - u^{n+1}_K) + q_j u^{n+1}_{\gamma,j}, \end{cases}$$

that discretize the following Robin quantities:

$$(14)\qquad \pm\frac{\partial v_j}{\partial x^{e_j}}(\delta,t) + q_j v_j(\delta,t) \text{ and } \pm\frac{1}{|\gamma_j|}\int_{\gamma_j}\frac{\partial u}{\partial n}(\cdot,t)d\gamma + q_j u(x,y,t)|_{\gamma_j}.$$

The notation for the Robin quantity is r when the normal derivative is directed from the 2D subdomain to the 1D subdomain, and r_- in the opposite direction. Note that a pointwise Robin interface condition for the 2D separated problem would be inconsistent with the transmission conditions, whether (3) or (4). The Robin condition must be a function of the mean value of the normal derivative.

Using (13), we can now reinterpret the fluxes defined by (7) and (11) by expressing them in terms of Robin quantities rather than solution values at the interfaces. More precisely, for $j = 1, ..., p$, if $q_j \neq -1/h^{e_j}_{1/2}$ and $q_j \neq -s\tau_j$, from (13) we deduce that

$$\begin{cases} v^{n+1}_{j,0} = \dfrac{v^{n+1}_{j,1} + h^{e_j}_{1/2} r^{n+1}_{-j}}{q_j h^{e_j}_{1/2} + 1}, \\ u^{n+1}_{\gamma,j} = \dfrac{r^{n+1}_{0j} + \frac{1}{|\gamma_j|}\sum_{\sigma\subset\gamma_j,\sigma\in\mathcal{E}_K}\frac{m(\sigma)}{d_\sigma}u^{n+1}_K}{q_j + s\tau_j}. \end{cases}$$

Then we can easily check that, for $j = 1, ..., p$,

$$(15)\qquad \begin{cases} F^{j,n+1}_{1/2} = -\dfrac{q_j v^{n+1}_{j,1} - r^{n+1}_{-j}}{q_j h^{e_j}_{1/2} + 1}, \\ r^{n+1}_j = \dfrac{q_j h^{e_j}_{1/2} - 1}{q_j h^{e_j}_{1/2} + 1} r^{n+1}_{-j} + \dfrac{2q_j}{q_j h^{e_j}_{1/2} + 1} v^{n+1}_{j,1}, \end{cases}$$

$$(16)\qquad \begin{cases} F^{n+1}_{K,\sigma} = -\dfrac{m(\sigma)}{d_\sigma}\left(\dfrac{r^{n+1}_{0j} + \frac{1}{|\gamma_j|}\sum_{\sigma\subset\gamma_j,\sigma\in\mathcal{E}_K}\frac{m(\sigma)}{d_\sigma}u^{n+1}_K}{q_j + s\tau_j} - u^{n+1}_K\right), \\ \forall\sigma\subset\gamma_j\ ,\ \sigma\in\mathcal{E}_K, \\ r^{n+1}_{-0j} = \dfrac{q_j - s\tau_j}{q_j + s\tau_j} r^{n+1}_{0j} + \dfrac{2q_j}{q_j + s\tau_j}\dfrac{1}{|\gamma_j|}\displaystyle\sum_{\sigma\subset\gamma_j,\sigma\in\mathcal{E}_K}\frac{m(\sigma)}{d_\sigma}u^{n+1}_K, \end{cases}$$

where

$$(17)\qquad s\tau_j = \frac{1}{|\gamma_j|}\sum_{\sigma\subset\gamma_j}\frac{m(\sigma)}{d_\sigma},$$

and that (12) is equivalent to

$$(18)\qquad r^{n+1}_{0j} = r^{n+1}_j, \text{ and } r^{n+1}_{-j} = r^{n+1}_{-0j}, j = 1, ..., p.$$

The linear system (6-15-8-16-18) has more equations and unknowns than (6-7-8-11-12), but the values of (u_K^n) and $(v_{j,i}^n)_{1\le i\le N_j}$ that are solutions are the same.

By ordering the equations and unknowns of (6-15-8-16-18), the system can be written in block form (see [21]). If p were equal to 1, we would obtain

$$\left(\begin{array}{c|c} A_0 & C_0 \\ \hline C_1 & A_1 \end{array}\right)\begin{pmatrix} \tilde{\boldsymbol{u}}^{n+1} \\ \tilde{\boldsymbol{v}}_{\boldsymbol{1}}^{n+1} \end{pmatrix} = \begin{pmatrix} \tilde{\boldsymbol{b}}_{\boldsymbol{0}}^{n} \\ \tilde{\boldsymbol{b}}_{\boldsymbol{1}}^{n} \end{pmatrix}, \tag{19}$$

with $\tilde{\boldsymbol{u}}^{n+1} = \begin{pmatrix} (u_K^{n+1}) \\ r_{01}^{n+1} \\ r_{-01}^{n+1} \end{pmatrix}$ and $\tilde{\boldsymbol{v}}_{\boldsymbol{1}}^{n+1} = \begin{pmatrix} r_1^{n+1} \\ r_{-1}^{n+1} \\ (v_{1,i}^{n+1}) \end{pmatrix}$. The equation $(18)_1$ (respectively $(18)_2$) is taken into account in the first (respectively second) line of blocks. The matrix C_0 has a single non-zero column, the first, which represents the influence of r_1^{n+1} on $\tilde{\boldsymbol{u}}^{n+1}$. The matrix C_1 has a single non-zero column, the last one, which represents the influence of r_{-01}^{n+1} on $\tilde{\boldsymbol{v}}_{\boldsymbol{1}}^{n+1}$. With p branches, instead of one, the unknowns are $\tilde{\boldsymbol{u}}^{n+1}$, $\tilde{\boldsymbol{v}}_{\boldsymbol{j}}^{n+1}$, $j=1,...,p$. This time all the $r_{0j}^{n+1}, r_{-0j}^{n+1}, j=1,...,p$, are taken into account in $\tilde{\boldsymbol{u}}^{n+1}$, and $\tilde{\boldsymbol{v}}_{\boldsymbol{j}}^{n+1}$ is obtained by replacing 1 by j in the above expression for $\tilde{\boldsymbol{v}}_{\boldsymbol{1}}^{n+1}$. The matrix C_0 has p non-zero columns E_{0j} (related to r_j^{n+1}), and the block row $(C_1|A_1)$ is replaced by p block rows $(C_j|A_j)$, where the matrices C_j have a single non-zero column E_j related to r_{-0j}^{n+1}, and A_j is related to $\tilde{\boldsymbol{v}}_{\boldsymbol{j}}^{n+1}, j=1,...,p$.

The iterative Schwarz method in volume to solve (1)"csa" can be written

$$\left\{\begin{array}{l} \tilde{\boldsymbol{u}}^{n+1,l+1} = A_0^{-1}(\tilde{\boldsymbol{b}}_{\boldsymbol{0}}^{n} - \sum_{j=1}^{p} E_{0j} r_j^{n+1,l}), \\ \tilde{\boldsymbol{v}}_{\boldsymbol{j}}^{n+1,l+1} = A_j^{-1}(\tilde{\boldsymbol{b}}_{\boldsymbol{j}}^{n} - E_j r_{-0j}^{n+1,l}), j=1,...,p, \end{array}\right. \tag{20}$$

where l is the iteration index. At the level of the transmission conditions (18), (20) means that

$$r_{0j}^{n+1,l+1} = r_j^{n+1,l} \text{ and } r_{-j}^{n+1,l+1} = r_{-0j}^{n+1,l}, j=1,...,p, \tag{21}$$

which are Robin boundary conditions for the 1D and 2D separated problems.

In particular, we deduce from (20) the substructured version of the iterative scheme, that is the following iterative scheme acting on variables defined exclusively on the interfaces:

$$\left\{\begin{array}{l} r_j^{n+1,l+1} - S_{1D,j}^{R_-R}(r_{-0j}^{n+1,l}) = 0, j=1,...,p, \\ (r_{-01}^{n+1,l+1},...,r_{-0p}^{n+1,l+1}) - S_{2D}^{RR_-}(r_1^{n+1,l},...,r_p^{n+1,l}) = 0, \end{array}\right. \tag{22}$$

where the operator $S_{1D,j}^{R_-R}$ from $I\!R$ to $I\!R$, $j\in\{1,...,p\}$, is defined by

$$\zeta_j \mapsto S_{1D,j}^{R_-R}(\zeta_j) = r_j^{n+1},$$

where r_j^{n+1} is given by $(15)_2$ with $(v_{j,i}^{n+1})$ solution of the 1D separated problem (6)-$(15)_1$ with the boundary condition $r_{-j}^{n+1} = \zeta_j$, and the operator $S_{2D}^{RR_-}$ from $I\!R^p$ to $I\!R^p$ is defined by

$$(\omega_1,...,\omega_p) \mapsto S_{2D}^{RR_-}(\omega_1,...,\omega_p) = (r_{-01}^{n+1},...,r_{-0p}^{n+1}),$$

where r_{-0j}^{n+1} is given by $(16)_2$ with (u_K^{n+1}) solution of the 2D separated problem (8)-$(16)_1$ with the boundary condition $r_{0j}^{n+1} = \omega_j, j=1,...,p$, that is well posed although it involves the mean value of the normal derivative, because the boundary condition necessarily implies that the solution is constant on the interface. Each operator is named according to its input (boundary conditions) and output (operator-supplied) values. Note also that in both cases, the normal derivative in the Robin type boundary condition is directed outward.

In practice, in the numerical tests, the substructured version of the iterative Schwarz method (22) is used as preconditioner for GMRES. That is to say we consider the fixed point limit of (22) that is

$$\left\{\begin{array}{l}\omega_j - S^{R_-R}_{1D,j}(\zeta_j) = 0, j = 1, ..., p,\\ (\zeta_1, ..., \zeta_p) - S^{RR_-}_{2D}(\omega_1, ..., \omega_p) = 0,\end{array}\right. \tag{23}$$

and we solve it by GMRES. Once $(\omega_j, \zeta_j), j = 1, ..., p$, have been determined, knowing that $\omega_j = r^{n+1}_j = r^{n+1}_{0j}$ and $\zeta_j = r^{n+1}_{-0j} = r^{n+1}_{-j}$, we obtain (u^{n+1}_K) and $(v^{n+1}_{j,i})$ by solving the 1D and 2D problems, which are then completely dissociated.

2.3. Continuity in average of the solution and continuity of the normal flux. Regarding the alternative problem (1)"dsa", the value of the solution is not assumed to be constant on the interfaces. The approximated value of the solution on the edge σ on the interface γ_j at time t_n is called $u^n_\sigma, \sigma \subset \gamma_j, j = 1, ..., p$, in [41], where the corresponding monolithic scheme is described. This is a value that can vary from edge to edge on the same interface γ_j. On the contrary, the transmission conditions (5) involve that the value of the normal derivative of the solution on the interface γ_j, $j = 1, ..., p$, on the $\Omega(0)$ side is constant. The monolithic scheme to solve (1)"dsa" is recalled. It includes (6)-(7)-(8), and:

$$F^n_{K,\sigma} = -\frac{m(\sigma)}{d_\sigma}(u^n_\sigma - u^n_K), \forall\sigma \subset \gamma_j\ ,\ \sigma \in \mathcal{E}_K, j = 1, ..., p, \tag{24}$$

$$\left\{\begin{array}{l}\dfrac{u^n_\sigma - u^n_K}{d_\sigma} = \dfrac{v^n_{j,1} - v^n_{j,0}}{h^{e_j}_{1/2}}, \forall\sigma \subset \gamma_j\ ,\ \sigma \in \mathcal{E}_K, j = 1, ..., p,\\ \dfrac{1}{\theta_j\varepsilon}\displaystyle\sum_{\sigma\subset\gamma_j,\sigma\in\mathcal{E}_K} m(\sigma)u^n_\sigma = v^n_{j,0}, j = 1, ..., p.\end{array}\right. \tag{25}$$

New variables are suitable for writing the Schwarz numerical scheme that discretizes (1)"dsa". Theses are the approximations of $\dfrac{\partial v_j}{\partial x^{e_j}}(\delta, t_{n+1})$ named $d^{n+1}_{j,0}$, and the approximations of $\dfrac{\partial u}{\partial n}(x, y, t_{n+1})$ for all $(x, y) \in \gamma_j$ named $d^{n+1}_{\gamma,j}, j = 1, ..., p$. The new equivalent description of the monolithic scheme is the following. This time, it involves taking equations (6) and (8) and supplementing them with:

$$F^{j,n+1}_{1/2} = -d^{n+1}_{j,0}, j = 1, ..., p, \tag{26}$$

$$F^{n+1}_{K,\sigma} = -m(\sigma)d^{n+1}_{\gamma,j}, \forall\sigma \subset \gamma_j\ , \sigma \in \mathcal{E}_K, j = 1, ..., p, \tag{27}$$

$$\left\{\begin{array}{l}d^{n+1}_{\gamma,j} = d^{n+1}_{j,0},\\ \dfrac{1}{|\gamma_j|}\displaystyle\sum_{\sigma\subset\gamma_j,\sigma\in\mathcal{E}_K} m(\sigma)u^{n+1}_K + \dfrac{d^{n+1}_{\gamma,j}}{|\gamma_j|}\sum_{\sigma\subset\gamma_j} m(\sigma)d_\sigma = v^{n+1}_{j,1} - h^{e_j}_{1/2}d^{n+1}_{j,0},\end{array}\right. \tag{28}$$

$j = 1, ..., p$.

Relations (26) and (27) discretize $-\dfrac{\partial v_j}{\partial x^{e_j}}(\delta, t_{n+1})$ and $-\displaystyle\int_\sigma \frac{\partial u}{\partial n}(\cdot, t_{n+1})d\gamma$. Relations (28) are the discretization of (4) and (5). To discretize (4), we might first use $(25)_2$, then replace u^{n+1}_σ and $v^{n+1}_{j,0}$ as a function of $u^{n+1}_K, d^{n+1}_{\gamma,j}, v^{n+1}_{j,1}$ and $d^{n+1}_{j,0}$, since the latter are unknowns in the system, whereas u^{n+1}_σ and $v^{n+1}_{j,0}$ are not.

Now, as before, we make a change of variable in the system. Its purpose is to introduce the Robin quantities needed to describe the interface conditions in the Schwarz method. About the Robin quantities defined in (13), r_j^{n+1} and r_{-j}^{n+1} do not change, but r_{0j}^{n+1} and r_{-0j}^{n+1} are quite different. For $j = 1, ..., p$, expressed in relation to the new variables $d_{j,0}^{n+1}$ and $d_{\gamma,j}^{n+1}$, where here

$$s\tau_j = \frac{|\gamma_j|}{\sum_{\sigma\subset\gamma_j} m(\sigma)d_\sigma}, \tag{29}$$

we have

$$\begin{cases} r_j^{n+1} &= (1 - q_j h_{1/2}^{e_j})d_{j,0}^{n+1} + q_j v_{j,1}^{n+1}, \\ r_{-j}^{n+1} &= -(1 + q_j h_{1/2}^{e_j})d_{j,0}^{n+1} + q_j v_{j,1}^{n+1}, \\ r_{0j}^{n+1} &= \frac{q_j + s\tau_j}{s\tau_j} d_{\gamma,j}^{n+1} + \frac{q_j}{|\gamma_j|}\sum_{\sigma\subset\gamma_j,\sigma\in\mathcal{E}_K} m(\sigma)u_K^{n+1}, \\ r_{-0j}^{n+1} &= \frac{q_j - s\tau_j}{s\tau_j} d_{\gamma,j}^{n+1} + \frac{q_j}{|\gamma_j|}\sum_{\sigma\subset\gamma_j,\sigma\in\mathcal{E}_K} m(\sigma)u_K^{n+1}, \end{cases} \tag{30}$$

that discretize this time:

$$\pm\frac{\partial v_j}{\partial x^{e_j}}(\delta, t) + q_j v_j(\delta, t) \text{ and } \pm\frac{\partial u}{\partial n}(x, y, t)|_{\gamma_j} + q_j\frac{1}{|\gamma_j|}\int_{\gamma_j} u(\cdot, t)d\gamma. \tag{31}$$

We change the unknowns $d_{j,0}^{n+1}$ and $d_{\gamma,j}^{n+1}$ as above. For $j = 1, ..., p$, with $q_j \neq -1/h_{1/2}^{e_j}$, $q_j \neq -s\tau_j$, we check that (15) is kept while (16) now becomes

$$\begin{cases} F_{K,\sigma}^{n+1} = -\dfrac{m(\sigma)s\tau_j}{q_j + s\tau_j}\left(r_{0j}^{n+1} - \dfrac{q_j}{|\gamma_j|}\displaystyle\sum_{\sigma\subset\gamma_j,\sigma\in\mathcal{E}_K} m(\sigma)u_K^{n+1}\right), \\ \forall\sigma\subset\gamma_j\ ,\ \sigma\in\mathcal{E}_K, \\ r_{-0j}^{n+1} = \dfrac{q_j - s\tau_j}{q_j + s\tau_j} r_{0j}^{n+1} - \dfrac{2q_j s\tau_j}{q_j + s\tau_j}\dfrac{1}{|\gamma_j|}\displaystyle\sum_{\sigma\subset\gamma_j,\sigma\in\mathcal{E}_K} m(\sigma)u_K^{n+1}. \end{cases} \tag{32}$$

We still have (28) equivalent to (18). By ordering the equations and unknowns exactly as it is done above for (1)"csa", we arrive at the same block form (19).

The iterative Schwarz method in volume to solve (1)"dsa" is exactly the same as (20) but this time the matrices are from (6-15-8-32-18). We still have (21). The substructured version of the iterative Schwarz method is again (22) and the fixed point limit is again (23), where the operator $S_{1D,j}^{R_-R}$ is defined above and $S_{2D}^{RR_-}$, from $\mathbb{R}^p$ to $\mathbb{R}^p$, is such that

$$(\omega_1, ..., \omega_p) \mapsto S_{2D}^{RR_-}(\omega_1, ..., \omega_p) = (r_{-01}^{n+1}, ..., r_{-0p}^{n+1}),$$

where r_{-0j}^{n+1} is given by $(32)_2$ with (u_K^{n+1}) solution of the 2D separated problem (8)-$(32)_1$ with the boundary condition $r_{0j}^{n+1} = \omega_j$.

3. Convergence

We prove that the iterative Schwarz method in substructured form that is (22) is convergent as soon as $q_j > 0, j = 1, ..., p$. We give the convergence proof by energy estimates.

3.1. Existence and uniqueness. Let us recall that the schemes (6-15-8-16-18) and (6-15-8-32-18) lead to linear systems

$$A\boldsymbol{U}^{n+1} = \boldsymbol{b}^n, \tag{33}$$

whose $\boldsymbol{U}^{n+1}$ is unknown, $n \in \{0, ..., N_k\}$, with

$$(\boldsymbol{U}^{n+1})^T = \left((\tilde{\boldsymbol{u}}^{n+1})^T, \{(\tilde{\boldsymbol{v}}_{\boldsymbol{j}}^{n+1})^T, \boldsymbol{j} = 1, ..., p\}\right).$$

A block decomposition of the elements A and $\boldsymbol{b}^n$ is given in (19) if $p=1$.
In the same way, let us denote $\boldsymbol{U}^{n+1,l}$ the lth iterate given by the iterative Schwarz method, with $(\boldsymbol{U}^{n+1,l})^T = \Big((\tilde{\boldsymbol{u}}^{n+1,l})^T, \{(\tilde{\boldsymbol{v}}_{\boldsymbol{j}}{}^{n+1,l})^T, \boldsymbol{j}=1,...,p\}\Big)$, and such that $\boldsymbol{U}^{n+1,l+1}$ is the unknown vector of a linear system in the form of

$$M\boldsymbol{U}^{n+1,l+1} = N\boldsymbol{U}^{n+1,l} + \boldsymbol{b}^n,$$

to which the algorithm (20) leads, where $A = M - N$ and

$$M = \left(\begin{array}{c|c} A_0 & 0 \\ \hline 0 & A_1 \end{array}\right), \qquad -N = \left(\begin{array}{c|c} 0 & C_0 \\ \hline C_1 & 0 \end{array}\right), \qquad \boldsymbol{b}^n = \begin{pmatrix} \tilde{\boldsymbol{b}}_{\boldsymbol{0}}{}^n \\ \tilde{\boldsymbol{b}}_{\boldsymbol{1}}{}^n \end{pmatrix}, \tag{34}$$

if $p=1$. We find the fact that the parallel Schwarz iterative method (20) is a block Jacobi method to solve (33).

3.1.1. Continuity of the solution and continuity in average of the normal flux.

Lemma 1. *Assuming $q_j > 0, j = 1,...,p$, the system (20) associated to (1)"csa" has a unique solution $\boldsymbol{U}^{n+1,l+1}$ for a given value of $\boldsymbol{U}^{n+1,l}$.*

Proof. To prove existence and uniqueness, it is sufficient to prove that M is regular. To do this, for a given $n \in \{0,...,N_k\}$, let us prove that $\boldsymbol{U}^{n+1,l+1} = 0$ if $\boldsymbol{U}^{n+1,l} = 0$ and $\boldsymbol{b}^n = 0$, that is $f_i^{e_j,n} = 0, v_{j,i}^n = 0, i = 1,...,N_j, j = 1,...,p,$ $f_K^n = 0, u_K^n = 0, K \in \mathcal{T}$.

Under this assumption, we multiply the coefficients of the equation $(6)_1$ by $v_{j,i}^{n+1,l+1}$, replacing the numerical fluxes by their values, and we sum over i, then we multiply by $|\gamma_j|$ and sum over j. This gives:

$$\begin{aligned} &\sum_{j=1}^{p} |\gamma_j| \sum_{i=1}^{N_j} h_i^{e_j} \frac{(v_{j,i}^{n+1,l+1})^2}{\Delta t} - \sum_{j=1}^{p} |\gamma_j| \left(\sum_{i=1}^{N_j} \frac{(v_{j,i+1}^{n+1,l+1} - v_{j,i}^{n+1,l+1}) v_{j,i}^{n+1,l+1}}{h_{i+1/2}^{e_j}} \right) \\ &+ \sum_{j=1}^{p} |\gamma_j| \left(\sum_{i=1}^{N_j} \frac{(v_{j,i}^{n+1,l+1} - v_{j,i-1}^{n+1,l+1}) v_{j,i}^{n+1,l+1}}{h_{i-1/2}^{e_j}} \right) = 0. \end{aligned} \tag{35}$$

Let $T1$, $T2$ and $T3$ be the three terms to the left of the equal sign above. In T_3, let us leave aside the term corresponding to $i=1$, increase the summation index i by 1 and remember that $v_{j,N_j+1}^{n+1,l+1} = 0, j = 1,...,p$. We see that terms of $T2$ and $T3$ factorize.

Then we multiply the coefficients of the equation $(8)_1$ by $u_K^{n+1,l+1}$, replacing again the numerical fluxes by their values, and we sum over $K \in \mathcal{T}$. This gives

$$\begin{aligned} &\sum_{K \in \mathcal{T}} \frac{m(K)}{\Delta t} (u_K^{n+1,l+1})^2 \\ &- \sum_{K \in \mathcal{T}} \sum_{\sigma \in \mathcal{E}_K, \sigma = \sigma_{K|L}} \frac{m(\sigma)}{d_\sigma} (u_L^{n+1,l+1} - u_K^{n+1,l+1}) u_K^{n+1,l+1} \\ &- \sum_{K \in \mathcal{T}} \sum_{j=1}^{p} \sum_{\sigma \in \mathcal{E}_K, \sigma \subset \gamma_j} \frac{m(\sigma)}{d_\sigma} (u_{\gamma,j}^{n+1,l+1} - u_K^{n+1,l+1}) u_K^{n+1,l+1} = 0. \end{aligned} \tag{36}$$

Let $Q1$, $Q2$ and $Q3$ be the three terms to the left of the equal sign above. We use the fact that $F_{K,\sigma}^{n+1,l+1} = -F_{L,\sigma}^{n+1,l+1}$ if $\sigma = \sigma_{K/L}$ to reorder the summation in $Q2$.

Summing (35) and (36), factorizing $T2$ and $T3$, and summing $Q2$ and $Q3$ over edges rather than control volumes, we have

$$\begin{aligned}
&\sum_{j=1}^{p}|\gamma_j|\sum_{i=1}^{N_j}\frac{h_i^{e_j}}{\Delta t}(v_{j,i}^{n+1,l+1})^2+\sum_{K\in\mathcal{T}}\frac{m(K)}{\Delta t}(u_K^{n+1,l+1})^2\\
&+\sum_{j=1}^{p}|\gamma_j|\left(\sum_{i=1}^{N_j}\frac{(v_{j,i+1}^{n+1,l+1}-v_{j,i}^{n+1,l+1})^2}{h_{i+1/2}^{e_j}}\right)\\
&+\sum_{j=1}^{p}|\gamma_j|\left(\frac{v_{j,1}^{n+1,l+1}-v_{j,0}^{n+1,l+1}}{h_{1/2}^{e_j}}(v_{j,1}^{n+1,l+1}-v_{j,0}^{n+1,l+1}+v_{j,0}^{n+1,l+1})\right)\\
&+\sum_{\sigma\in\mathcal{E}_{int},\sigma=\sigma_{K|L}}\frac{m(\sigma)}{d_\sigma}(u_K^{n+1,l+1}-u_L^{n+1,l+1})^2\\
&+\sum_{j=1}^{p}\sum_{\sigma\subset\gamma_j,\sigma\in\mathcal{E}_K}\frac{m(\sigma)}{d_\sigma}(u_{\gamma,j}^{n+1,l+1}-u_K^{n+1,l+1})(u_{\gamma,j}^{n+1,l+1}-u_K^{n+1,l+1}-u_{\gamma,j}^{n+1,l+1})\\
&=0.
\end{aligned}\tag{37}$$

Let us now define

$$\begin{aligned}
L_{l+1}:=&\sum_{j=1}^{p}|\gamma_j|\sum_{i=1}^{N_j}\frac{h_i^{e_j}}{\Delta t}(v_{j,i}^{n+1,l+1})^2+\sum_{K\in\mathcal{T}}\frac{m(K)}{\Delta t}(u_K^{n+1,l+1})^2\\
&+\sum_{j=1}^{p}|\gamma_j|\left(\sum_{i=0}^{N_j}\frac{(v_{j,i+1}^{n+1,l+1}-v_{j,i}^{n+1,l+1})^2}{h_{i+1/2}^{e_j}}\right)\\
&+\sum_{\sigma\in\mathcal{E}_{int},\sigma=\sigma_{K|L}}\frac{m(\sigma)}{d_\sigma}(u_K^{n+1,l+1}-u_L^{n+1,l+1})^2\\
&+\sum_{j=1}^{p}\sum_{\sigma\subset\gamma_j,\sigma\in\mathcal{E}_K}\frac{m(\sigma)}{d_\sigma}(u_{\gamma,j}^{n+1,l+1}-u_K^{n+1,l+1})^2.
\end{aligned}\tag{38}$$

We deduce from (37) that

$$\begin{aligned}
L_{l+1}=&-\sum_{j=1}^{p}|\gamma_j|\frac{v_{j,1}^{n+1,l+1}-v_{j,0}^{n+1,l+1}}{h_{1/2}^{e_j}}v_{j,0}^{n+1,l+1}\\
&+\sum_{j=1}^{p}\sum_{\sigma\subset\gamma_j,\sigma\in\mathcal{E}_K}\frac{m(\sigma)}{d_\sigma}(u_{\gamma,j}^{n+1,l+1}-u_K^{n+1,l+1})u_{\gamma,j}^{n+1,l+1}.
\end{aligned}\tag{39}$$

Using (13), we find that

$$\begin{aligned}
L_{l+1}\quad&=-\sum_{j=1}^{p}|\gamma_j|\frac{r_j^{n+1,l+1}-r_{-j}^{n+1,l+1}}{2}\,\frac{r_j^{n+1,l+1}+r_{-j}^{n+1,l+1}}{2q_j}\\
&+\sum_{j=1}^{p}|\gamma_j|\frac{r_{0j}^{n+1,l+1}-r_{-0j}^{n+1,l+1}}{2}\,\frac{r_{0j}^{n+1,l+1}+r_{-0j}^{n+1,l+1}}{2q_j}\\
&=-\sum_{j=1}^{p}|\gamma_j|\frac{(r_j^{n+1,l+1})^2-(r_{-j}^{n+1,l+1})^2}{4q_j}\\
&+\sum_{j=1}^{p}|\gamma_j|\frac{(r_{0j}^{n+1,l+1})^2-(r_{-0j}^{n+1,l+1})^2}{4q_j}.
\end{aligned}\tag{40}$$

It can be deduced from (21) that

$$(41)\quad L_{l+1} = -\sum_{j=1}^{p} |\gamma_j| \frac{(r_j^{n+1,l+1})^2 - (r_{\_0j}^{n+1,l})^2}{4q_j} + \sum_{j=1}^{p} |\gamma_j| \frac{(r_j^{n+1,l})^2 - (r_{\_0j}^{n+1,l+1})^2}{4q_j}.$$

Since $\boldsymbol{U}^{n+1,l} = 0$, we conclude that L_{l+1} is equal to a term small than zero. But being L_{l+1} defined as the sum of positive terms, it follows that all terms are zero, which implies that $\boldsymbol{U}^{n+1,l+1} = 0$. □

3.1.2. Continuity in average of the solution and continuity of the normal flux.

Lemma 2. *Assuming $q_j > 0, j = 1, ..., p$, the system (20) associated to (1)"dsa" has a unique solution $\boldsymbol{U}^{n+1,l+1}$ for a given value of $\boldsymbol{U}^{n+1,l}$.*

Proof. The proof is similar to the previous one. It is sufficient to repeat it when replacing the fluxes by their value in $(6)_1$ and $(8)_1$. Let us now write the counterpart of (35) and (36). The interior fluxes are unchanged. Only the flux values at the interfaces $\gamma_j, j = 1, ..., p$, change. The similarity between the two proofs can be clearly seen by keeping $v_{j,0}^{n+1,l+1}$ and simply replacing $u_{\gamma,j}^{n+1,l+1}$ by $u_\sigma^{n+1,l+1}$, which is a value that can vary from edge to edge on the same interface γ_j in the "dsa" model. However, the proof is more direct here if we use $d_{j,0}^{n+1,l+1}$ and $d_{\gamma,j}^{n+1,l+1}$, which are unknowns in the system.

$$(42)\quad \begin{aligned} &\sum_{j=1}^{p} |\gamma_j| \sum_{i=1}^{N_j} h_i^{e_j} \frac{(v_{j,i}^{n+1,l+1})^2}{\Delta t} - \sum_{j=1}^{p} |\gamma_j| \left(\sum_{i=1}^{N_j} \frac{(v_{j,i+1}^{n+1,l+1} - v_{j,i}^{n+1,l+1}) v_{j,i}^{n+1,l+1}}{h_{i+1/2}^{e_j}} \right) \\ &+ \sum_{j=1}^{p} |\gamma_j| \left(\sum_{i=2}^{N_j} \frac{(v_{j,i}^{n+1,l+1} - v_{j,i-1}^{n+1,l+1}) v_{j,i}^{n+1,l+1}}{h_{i-1/2}^{e_j}} \right) \\ &+ \sum_{j=1}^{p} |\gamma_j| d_{j,0}^{n+1,l+1} v_{j,1}^{n+1,l+1} = 0, \end{aligned}$$

and

$$(43)\quad \begin{aligned} &\sum_{K\in\mathcal{T}} \frac{m(K)}{\Delta t} (u_K^{n+1,l+1})^2 \\ &- \sum_{K\in\mathcal{T}} \sum_{\sigma\in\mathcal{E}_K, \sigma=\sigma_{K|L}} \frac{m(\sigma)}{d_\sigma} (u_L^{n+1,l+1} - u_K^{n+1,l+1}) u_K^{n+1,l+1} \\ &- \sum_{K\in\mathcal{T}} \sum_{j=1}^{p} \sum_{\sigma\in\mathcal{E}_K, \sigma\subset\gamma_j} m(\sigma) d_{\gamma,j}^{n+1,l+1} u_K^{n+1,l+1} = 0. \end{aligned}$$

Then, as before, comes

$$
\begin{aligned}
&\sum_{j=1}^{p}|\gamma_j|\sum_{i=1}^{N_j}\frac{h_i^{e_j}}{\Delta t}(v_{j,i}^{n+1,l+1})^2+\sum_{K\in\mathcal{T}}\frac{m(K)}{\Delta t}(u_K^{n+1,l+1})^2\\
&+\sum_{j=1}^{p}|\gamma_j|\left(\sum_{i=1}^{N_j}\frac{(v_{j,i+1}^{n+1,l+1}-v_{j,i}^{n+1,l+1})^2}{h_{i+1/2}^{e_j}}\right)\\
&+\sum_{j=1}^{p}|\gamma_j|d_{j,0}^{n+1,l+1}(v_{j,1}^{n+1,l+1}-h_{1/2}^{e_j}d_{j,0}^{n+1,l+1}+h_{1/2}^{e_j}d_{j,0}^{n+1,l+1})\\
&+\sum_{\sigma\in\mathcal{E}_{int},\sigma=\sigma_{K|L}}\frac{m(\sigma)}{d_\sigma}(u_K^{n+1,l+1}-u_L^{n+1,l+1})^2\\
&-\sum_{K\in\mathcal{T}}\sum_{j=1}^{p}d_{\gamma,j}^{n+1,l+1}\left(\sum_{\sigma\in\mathcal{E}_K,\sigma\subset\gamma_j}m(\sigma)u_K^{n+1,l+1}+\alpha_j d_{\gamma,j}^{n+1,l+1}-\alpha_j d_{\gamma,j}^{n+1,l+1}\right)\\
&=0,
\end{aligned}
\tag{44}
$$

with $\alpha_j=\sum_{\sigma\subset\gamma_j}m(\sigma)d_\sigma$. The expressions introduced above simply correspond to those found in (28), and approximate the value of v_j and the average value of u on the interfaces.

The counterpart of L_{l+1} in the "dsa" context is

$$
\begin{aligned}
L_{l+1}:=&\sum_{j=1}^{p}|\gamma_j|\sum_{i=1}^{N_j}\frac{h_i^{e_j}}{\Delta t}(v_{j,i}^{n+1,l+1})^2+\sum_{K\in\mathcal{T}}\frac{m(K)}{\Delta t}(u_K^{n+1,l+1})^2\\
&+\sum_{j=1}^{p}|\gamma_j|\sum_{i=1}^{N_j}\frac{(v_{j,i+1}^{n+1,l+1}-v_{j,i}^{n+1,l+1})^2}{h_{i+1/2}^{e_j}}\\
&+\sum_{j=1}^{p}|\gamma_j|h_{1/2}^{e_j}(d_{j,0}^{n+1,l+1})^2\\
&+\sum_{\sigma\in\mathcal{E}_{int},\sigma=\sigma_{K|L}}\frac{m(\sigma)}{d_\sigma}(u_K^{n+1,l+1}-u_L^{n+1,l+1})^2\\
&+\sum_{K\in\mathcal{T}}\sum_{j=1}^{p}(\sum_{\sigma\subset\gamma_j}m(\sigma)d_\sigma)(d_{\gamma,j}^{n+1,l+1})^2.
\end{aligned}
\tag{45}
$$

We have

$$
\begin{aligned}
L_{l+1}=&-\sum_{j=1}^{p}|\gamma_j|d_{j,0}^{n+1,l+1}(v_{j,1}^{n+1,l+1}-h_{1/2}^{e_j}d_{j,0}^{n+1,l+1})\\
&+\sum_{K\in\mathcal{T}}\sum_{j=1}^{p}d_{\gamma,j}^{n+1,l+1}\left(\sum_{\sigma\in\mathcal{E}_K,\sigma\subset\gamma_j}m(\sigma)u_K^{n+1,l+1}+(\sum_{\sigma\subset\gamma_j}m(\sigma)d_\sigma)d_{\gamma,j}^{n+1,l+1}\right).
\end{aligned}
$$

Using (30) to express $d_{j,0}^{n+1,l+1}$ and $d_{\gamma,j}^{n+1,l+1}$ as a function of $r_j^{n+1,l+1}$, $r_{-j}^{n+1,l+1}$, $r_{0j}^{n+1,l+1}$ and $r_{-0j}^{n+1,l+1}$, we then find exactly the expression (40). We conclude as above.

□

3.2. Convergence of the algorithm.

Lemma 3. *Assuming $q_j > 0, j = 1, ..., p$, the vector $\boldsymbol{U}^{n+1,l}$ defined by the Schwarz algorithm (20) associated to (1)"csa" (respectively (1)"dsa") converges to the solution $\boldsymbol{U}^{n+1}$ of the hybrid scheme (6-15-8-16-18) (respectively (6-15-8-32-18)).*

Proof. The proof of convergence follows the main thread described in [8].

Using the same notation as in paragraph 3.1, we prove that $\boldsymbol{U}^{n+1,l+1}$ tends to $\boldsymbol{U}^{n+1}$ one term at a time when l tends to infinity.

Note that $M(\boldsymbol{U}^{n+1,l+1}-\boldsymbol{U}^{n+1}) = N(\boldsymbol{U}^{n+1,l}-\boldsymbol{U}^{n+1})$, that is $\boldsymbol{U}^{n+1,l+1}-\boldsymbol{U}^{n+1}$ is solution of (20) with a right hand side $\boldsymbol{b}^n$ equal to zero. So proving that $\boldsymbol{U}^{n+1,l+1} - \boldsymbol{U}^{n+1}$ tends to zero is equivalent to proving that the solution of (20) with a right hand side $\boldsymbol{b}^n$ equal to zero tends to zero.

Using the results and notations from the previous paragraphs, assuming $\boldsymbol{b}^n = 0$, it can be deduced from (41) that $L_{l+1} = E_l - E_{l+1}$ with

$$E_l = \sum_{j=1}^{p} \frac{|\gamma_j|}{4q_j}\left(r_j^{n+1,l}\right)^2 + \sum_{j=1}^{p} \frac{|\gamma_j|}{4q_j}\left(r_{-0j}^{n+1,l}\right)^2.$$

By definition $L_l \geq 0$. Moreover $\sum_{l=1}^{N} L_l = E_0 - E_N \leq E_0$ for all $N \geq 1$, because $E_l \geq 0$ for all l. The sequence of partial sums is increasing and bounded, so the series $\sum_{l=1}^{\infty} L_l$ is convergent. We deduce that L_l tends necessarily to zero as l tends to infinity, and so that each component of $\boldsymbol{U}^{n+1,l+1}$ tends to zero as l tends to infinity (from (38) and (13) for (1)"csa", and from (45) and (30) for (1)"dsa"). □

Given that the values of (u_K^n) and $(v_{j,i}^n)_{1\leq i\leq N_j}$ that are solutions of (6-15-8-16-18) and (6-7-8-11-12) are the same, the Schwarz algorithm (20) associated to (1)"csa" provides the solution to the monolithic scheme (6-7-8-11-12) defined at the start. The same can be said about the Schwarz algorithm (20) associated to (1)"dsa" and the values of (u_K^n) and $(v_{j,i}^n)_{1\leq i\leq N_j}$ as solutions to (6-26-8-27-28).

3.3. Interface system solver.

Theorem 4. *Assuming $q_j > 0, j = 1, ..., p$, the iterative Schwarz method in sub-structured form (22) is convergent. The method converges towards approximations of Robin-type quantities (14) (respectively (31)) given by the hybrid scheme (6-15-8-16-18) to solve (1)"csa" (respectively (6-15-8-32-18) to solve (1)"dsa").*

Proof. Lemma 3 states that the iterative Schwarz method (20) is convergent as soon as $q_j > 0, j = 1, ..., p$. Taking the iterative Schwarz method as a block Jacobi algorithm, as described in paragraph 3.1, we obtain by replacing N by $M - A$:

$$\begin{aligned} \boldsymbol{U}^{n+1,l+1} &= \boldsymbol{U}^{n+1,l} + M^{-1}(\boldsymbol{b}^n - A\boldsymbol{U}^{n+1,l}) \\ &= (I_d - M^{-1}A)\boldsymbol{U}^{n+1,l} + M^{-1}\boldsymbol{b}^n, \end{aligned} \tag{46}$$

where I_d is the identity matrix of the same size as A. We have

$$M^{-1} = \sum_{j=0}^{p} Q_j^T A_j^{-1} Q_j,$$

where Q_0 is the matrix of the operator which restricts to the variables of $\Omega(0)$ including r_{0j}^{n+1} and r_{-0j}^{n+1}, and Q_j to the variables of S_j including r_j^{n+1} and r_{-j}^{n+1}, $j = 1, ..., p$. The matrices Q_j are such that $\sum_{j=0}^{p} Q_j^T Q_j = I_d$.

Closely related to the discretized classical parallel Schwarz method, the restricted additive Schwarz (RAS) algorithm is a variant of the additive Schwarz method that improves on the convergence. It is introduced in [7]. In [9] the authors provide an algebraic characterization of RAS that includes (46). The proof of Theorem 4 thus follows from the proof of Theorem 1 [9] that establishes the equivalence between RAS and a substructured version of RAS.

□

The convergence of the GMRES method to solve (23) follows since it converges faster than the iterative Schwarz method in substructured form that is just the Jacobi method (see e.g. [10]). The GMRES method to solve (23) converges after only $2p$ iterations. All numerical tests are performed by solving the system (23) using GMRES. Though, the iterative Schwarz method is particularly useful to obtain a convergence result.

We do not deal with the iterative Schwarz method (46) considered as preconditioner for GMRES, i.e. we do not solve $M^{-1}A\boldsymbol{U}^{n+1} = M^{-1}\boldsymbol{b}^n$ directly with GMRES, in the numerical experiments, since this would imply computations with matrices at the volume level. It is proved for instance in [9] by introducing a substructured version of RAS to solve a linear problem, that, when used as preconditioners for GMRES, this substructured version is computationally less expensive and needs less memory than the classical version that gives the volume solution.

4. Numerical experiments

4.1. Introduction.

4.1.1. The model problems and the discretization. We solve (1)"csa" and (1)"dsa" in a domain D_ε (see Figure 2), with one node and two branches ($p = 2$), with $\theta_1 = \theta_2 = 1, \varepsilon = 0.2$, $l_1 = l_2 = 1$, $\delta = 0.5$, with the initial condition equal to zero and with $T = 0.5$. The problem that is solved is related to a polynomial

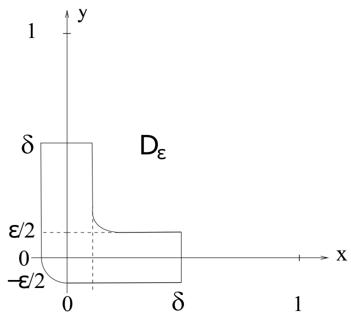

FIGURE 2. Numerical domain.

right-hand side. The f function is zero. Let (x, y) denote the coordinates in the canonical basis of $\mathbb{R}^2$, f_1 and f_2 are defined by

$$\begin{cases} f_1(x,y,t) = 5.10^7\,(x-0.5)^3\,(x-0.9)^3\,t^4 \\ -6.10^7\,(t-0.5)^5\,(x-0.5)\,(x-0.9)\,(5x^2-7x+2.41) \quad \text{if } 0.5 < x < 0.9, \end{cases}$$

$$\begin{cases} f_2(x,y,t) = 5.10^7\,(y-0.4)^3\,(y-0.8)^3\,t^4 \\ -6.10^7\,(t-0.5)^5\,(y-0.4)\,(y-0.8)\,(5y^2-6y+1.76) \quad \text{if } 0.4 < y < 0.8. \end{cases}$$

The tests are done with $\Delta t = 0.002$ (250 time iterations). The size of the mesh $\mathcal{T}$, that is the largest diameter of the control volumes, is equal to $h = 0.02$, which corresponds to 1684 control volumes. The mesh of S_j is uniform, with $x^{e_j}_{i+1/2} = \delta + i\,h$, and the points $x^{e_j}_i = \delta + i\,h/2, i = 0, ..., N_j, j = 1, 2$.

We compare the approximated solutions of (1)"csa" and (1)"dsa" obtained by using the substructured version of the iterative Schwarz method accelerated by GMRES with those obtained by the monolithic schemes, by calculating the L^2 norm of the difference at the final time $T = 0.5$. We use the basic GMRES algorithm, without the restarting option. The initial guess is equal to zero.

4.1.2. Diagonal preconditioning. Given that the interface system is only 4×4 size ($2p = 4$), convergence of GMRES is reached after 4 iterations. However, if the chosen tolerance is large, it happens that the resolution process may be stopped as early as the 2nd or 3rd iteration, because the norm of the residual is sufficiently small. This can happen for a single, 10, 50 or even 250 iterations in time. These inaccurate results can then accumulate to significantly distort the final result. For illustration, with $q = 50$ for (1)"csa", all 250 iterations in time converge with non-zero relative residuals with the tolerance 10^{-6} and we obtain a final L^2 error that is as large as $1.9\,10^{-6}$.

We propose here a preconditioning that allows obtaining a final L^2 error of order 10^{-13} or 10^{-14} even with a large tolerance. The construction of the preconditioning follows the same steps used to define the volumetric version (20), then the substructured version (22).

The linear system of the Schwarz scheme is obtained from (6-15-8-18) and (16) (respectively (32)) to solve (1)"csa" (respectively (1)"dsa") by introducing the variables ω_j and ζ_j (double trace formulation, see for instance [28]) which break down the equalities of (18) into

$$r^{n+1}_{0j} = \omega_j, r^{n+1}_j = \omega_j, \text{ and } r^{n+1}_{-j} = \zeta_j, r^{n+1}_{-0j} = \zeta_j, j = 1, ..., p.$$

These linear systems can be written in block form by grouping together the coefficients of the interface variables ω_j and ζ_j, as it is done for instance in [38]. With $\boldsymbol{u}^{n+1} = (u^{n+1}_K)$, $(\boldsymbol{u_\gamma}^{n+1})^T = (\omega_1\ \zeta_1\ \omega_2\ \zeta_2)$, $\boldsymbol{v_j}^{n+1} = (v^{n+1}_{j,i}), j = 1, 2$, this block form is

$$\begin{pmatrix} A_{00} & 0 & 0 & A_{0\gamma} \\ 0 & A_{11} & 0 & A_{1\gamma} \\ 0 & 0 & A_{22} & A_{2\gamma} \\ A_{\gamma 0} & A_{\gamma 1} & A_{\gamma 2} & A_{\gamma\gamma} \end{pmatrix} \begin{pmatrix} \boldsymbol{u}^{n+1} \\ \boldsymbol{v_1}^{n+1} \\ \boldsymbol{v_2}^{n+1} \\ \boldsymbol{u_\gamma}^{n+1} \end{pmatrix} = \begin{pmatrix} \boldsymbol{b_0}^n \\ \boldsymbol{b_1}^n \\ \boldsymbol{b_2}^n \\ \boldsymbol{0} \end{pmatrix}. \tag{47}$$

The lines of blocks from top to bottom correspond to (8)-$(16)_1$ then to (6)-$(15)_1$, $j = 1, 2$, for (1)"csa", and $(32)_1$ instead of $(16)_1$ for (1)"dsa". The last line corresponds to $(15)_2$-$(16)_2$ for (1)"csa", reformulated as

$$\begin{cases} -\dfrac{2q_j}{q_j h^{e_j}_{1/2} + 1} v^{n+1}_{j,1} + \omega_j - \dfrac{q_j h^{e_j}_{1/2} - 1}{q_j h^{e_j}_{1/2} + 1} \zeta_j = 0, \\ -\dfrac{2q_j}{q_j + s\tau_j} \dfrac{1}{|\gamma_j|} \displaystyle\sum_{\sigma \subset \gamma_j, \sigma \in \mathcal{E}_K} \dfrac{m(\sigma)}{d_\sigma} u^{n+1}_K - \dfrac{q_j - s\tau_j}{q_j + s\tau_j} \omega_j + \zeta_j = 0, \end{cases} \tag{48}$$

and to $(15)_2$-$(32)_2$ for (1)"dsa", reformulated as $(48)_1$ unchanged and

$$-\frac{2q_j s\tau_j}{q_j + s\tau_j} \frac{1}{|\gamma_j|} \sum_{\sigma \subset \gamma_j, \sigma \in \mathcal{E}_K} m(\sigma) u^{n+1}_K - \frac{q_j - s\tau_j}{q_j + s\tau_j} \omega_j + \zeta_j = 0, \tag{49}$$

for $j = 1$ then for $j = 2$. For illustration, in matrix form, we obtain

$$A_{\gamma\gamma} = \begin{pmatrix} 1 & -\dfrac{q_1 h_{1/2}^{e_1} - 1}{q_1 h_{1/2}^{e_1} + 1} & 0 & 0 \\ -\dfrac{q_1 - s\tau_1}{q_1 + s\tau_1} & 1 & 0 & 0 \\ 0 & 0 & 1 & -\dfrac{q_2 h_{1/2}^{e_2} - 1}{q_2 h_{1/2}^{e_2} + 1} \\ 0 & 0 & -\dfrac{q_2 - s\tau_2}{q_2 + s\tau_2} & 1 \end{pmatrix}.$$

We propose preconditioning (23) by a block diagonal matrix $B = \begin{pmatrix} B^1 & 0 \\ 0 & B^2 \end{pmatrix}$ where B^j are 2×2 diagonal matrices such that B^j_{11} acts on $(48)_1$ (Robin quantities on the 1D side) and B^j_{22} acts on $(48)_2$ or (49) (Robin quantities on the 2D side). The preconditioning consists in making one coefficient per line of $A_{\gamma\gamma}$ equal to 1 (the same choice for $j = 1$ and $j = 2$). The preconditioned versions of the scheme are referred to as variant: $\omega - \omega$, $\zeta - \omega$, and $\zeta - \zeta$, by listing the variables assigned a coefficient equal to one, first in $(48)_1$, and second in $(48)_2$ or (49). The original Schwarz interface systems (23), that leave the matrix $A_{\gamma\gamma}$ unchanged, are also referred to as variants $\omega - \zeta$. Note that the original schemes are defined for any $q_j > 0$, which is not the case for the other variants.

4.1.3. Robin parameters. Regarding the Robin parameters, for the sake of simplicity, it is assumed that $q_1 = q_2 = q$.

We remind that $s\tau_j$ is defined by (17) for (1)"csa" and (29) for (1)"dsa". Remembering that $|\gamma_j| = \sum_{\sigma \subset \gamma_j} m(\sigma), j = 1, ..., p$, it is easily proved with the help of the Cauchy-Schwarz-Buniakowski inequality that we have

Lemma 5. *The value of $s\tau_j$ from (29) for "dsa" is always smaller than the value of $s\tau_j$ from (17) for "csa", that is*

$$\frac{|\gamma_j|}{\sum_{\sigma \subset \gamma_j} m(\sigma) d_\sigma} \leq \frac{1}{|\gamma_j|} \sum_{\sigma \subset \gamma_j} \frac{m(\sigma)}{d_\sigma}, j = 1, ..., p.$$

The mesh is such that $s\tau_1 \simeq 243, s\tau_2 \simeq 204$ for "dsa", and $s\tau_1 \simeq 392, s\tau_2 \simeq 287$ for "csa". Below, error curves are supplied for values of q between 0 and 200, from 10 to 10, $q \neq 0$. The values $s\tau_j$ for which, depending on the variant, the interface systems may not be defined, are therefore not within the study range.

4.2. The Schwarz scheme to solve (1)"csa". Let us consider the original Schwarz interface system relating to (1)"csa" (variant $\omega - \zeta$). Figure 3 on the left shows a graphical representation of the errors obtained for $q = 1$, $q = 10i$ with $i \in \{1, ..., 40\}$, $q = 21$, $q = 22$, when the tolerance is 10^{-6}, 10^{-8}, and 10^{-10}. When solving the interface system by GMRES, we observe a number of time iterations for which the GMRES process stops before the 4th iteration and converges with a non-zero relative residual: for all values of q when the tolerance is 10^{-6}, for all values of q (but for a single time iteration) when the tolerance is 10^{-8}, and essentially when $q \approx 20$ when the tolerance is 10^{-10}. By testing integer values close to $q = 20$, we find that the error is greatest in this zone when $q = 22$ and that the tolerance must be as small as 10^{-12} to obtain convergence without non-zero relative residual when $q = 22$ with an error of $7.2\,10^{-14}$. At this tolerance level, the results are as uniformly accurate as if the interface system were solved by a direct method.

Variants $\omega-\omega$ and $\zeta-\omega$ give a minimal final error with a greater tolerance than with the original scheme. The variant $\omega-\omega$ is such that $B_{11}^{j}=1$ and $B_{22}^{j}=-\dfrac{q_j+s\tau_j}{q_j-s\tau_j}, j=1,2$. It is well defined if $q_j\neq s\tau_j, j=1,2$. The coefficients of B are arguably effective because they affect not only the weight between the separated problems in a given branch but also the weight between the two branches (since $s\tau_1\neq s\tau_2$). The same coefficients B_{22}^{j} act in the same way for variant $\zeta-\omega$, but this time $B_{11}^{j}=-\dfrac{q_jh_{1/2}^{e_j}+1}{q_jh_{1/2}^{e_j}-1}$, and it is not defined if $q_j=\dfrac{1}{h_{1/2}^{e_j}}=100$. The results, similar or even less accurate when $q=100$, are not detailed. The $\zeta-\zeta$ variant offers no improvement over variant $\omega-\zeta$, since $B_{22}^{j}=1$ has no effect and B_{11}^{j} excludes an additional $q=100$ value too.

Looking at the same range of values of q as above, we see from Figure 3 on the right that the variant $\omega-\omega$ gives results with tolerance 10^{-6} that are as accurate as the results of the original Schwarz scheme with tolerance 10^{-10} (see Figure 3 left) for all values $q>70$. When the tolerance is smaller, the behavior of both variants is the same. The same difficulty as above arises when $q=22$ as shown in Figure 3 right. When $q=22$, only a tolerance as small as 10^{-12} gives GMRES convergence without non-zero relative residual, the final error is then $1.3\,10^{-13}$.

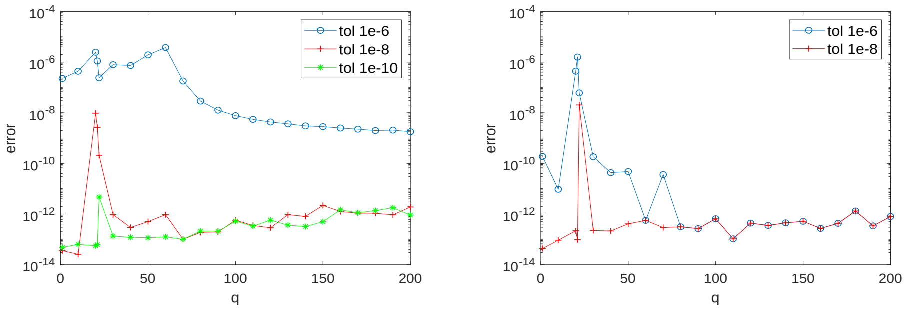

FIGURE 3. Difference between the monolithic solution and the solution given by the Schwarz scheme for (1)"csa". Variant $\omega-\zeta$ on the left, with tolerance 10^{-6} (blue), 10^{-8} (red), 10^{-10} (green). Variant $\omega-\omega$ on the right, with tolerance 10^{-6} (blue), 10^{-8} (red).

4.3. The Schwarz scheme to solve (1)"dsa". Now we consider the Schwarz interface system also described by (23) to solve (1)"dsa". Remember that operators $S_{1D,j}^{R_-R}$ are unchanged from the definition of the interface system for "csa", but operator $S_{2D}^{RR_-}$ is specifically defined.

As in the case of problem (1)"csa", the $\omega-\omega$ variant provides the most accurate results the fastest (for the largest tolerance). From Figure 4 on the left we see the errors obtained for $q=1$, $q=10i$ with $i\in\{1,...,40\}$, $q=21$, $q=22$, when the tolerance is 10^{-6} and 10^{-8}. We remind that the interface system is well defined if $q_j\neq s\tau_j, j=1,2$. You have to be careful that $s\tau_j$ does not have the same meaning as above: (29) for "dsa", and (17) for "csa". We merely point out that $s\tau_2$ is located right at the upper limit of tested values ($0<q_j\leq 200$), this induces inaccuracy. Nevertheless, the perturbation generated when $q=200\approx s\tau_2$ is very circumscribed and only observable with the greatest tolerance. On the contrary

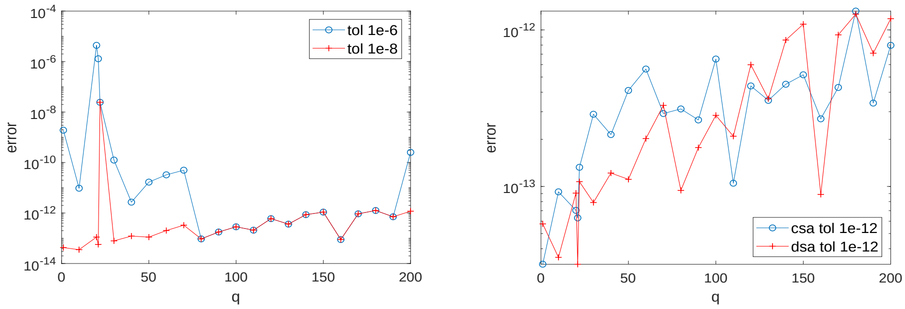

Figure 4. Difference between the monolithic solution and the solution given by the variant $\omega - \omega$ of Schwarz scheme for (1)"dsa" on the left, with tolerance 10^{-6} (blue), 10^{-8} (red). Difference between the monolithic solutions and the solutions given by Schwarz scheme for (1)"csa" (blue) and (1)"dsa" (red) with tolerance 10^{-12} on the right.

the values of $s\tau_j$ for "csa" are outside the range we are studying and therefore do not induce any alteration. When the tolerance is 10^{-6}, GMRES converges without non-zero relative residual for all values $q > 70$. The tolerance 10^{-8} is still not small enough to obtain accurate results for $q \approx 20$. Again, the tolerance must be as small as 10^{-12} to obtain convergence when $q = 22$ with an error of $1.1\,10^{-13}$.

Finally, we compare the results obtained with the variants $\omega - \omega$ of the Schwarz schemes to solve (1)"csa" and (1)"dsa" in Figure 4 on the right. The tolerance is 10^{-12} to be able to make a comparison between values that have been calculated with a high degree of accuracy. Even if the scale of the figure increases the gaps, the final L^2 error when the junction is discontinuous (red graph) is of the same order as when the junction is continuous (blue graph). The two schemes behave in the same way. The maximum L^2 error observed among the q values tested (for both types of transmission condition) is of order 10^{-12}, which is still very small. These results confirm the interest of the method.

5. Conclusion

In this paper, the solving of a condensed version of the heat equation set in a geometrical multi-scale domain is considered. The domain consists of a 2D central node and several 1D branches. Two kinds of physical transmission conditions between the 1D domains and the 2D domain are examined: continuity of the solution and of the mean value of its normal derivative, and continuity of the normal derivative of the solution and of the mean value of the solution itself. The iterative Schwarz method is generalized to solve the model problem and the convergence to the solution given by the monolithic scheme is proved in each case.

The solutions given by the iterative Schwarz method in substructured form and accelerated by GMRES are compared with those given by the monolithic schemes. We propose variants of the schemes obtained by preconditioning to achieve a minimal error of the difference at the final time with GMRES even when the tolerance is large.

From a numerical point of view, we do not observe any significant difference in behavior between the two coupling conditions.

Acknowledgments

The author would like to thank the associate editor and the referees for their pertinent advice, which enabled her to considerably improve the document. The present work is partially supported by the Research Federative Structures MODMAD FED 4169.

References

[1] Achdou, Y., Japhet, C., Maday, Y. and Nataf, F., A new cement to glue non-conforming grids with Robin interface conditions: the finite volume case, Numer. Math., 92(2002): 593-620.

[2] Alonso-Rodriguez, A. and Gerardo-Giorda, L., New non-overlapping domain decomposition methods for the time-harmonic Maxwell system, SIAM J. Sci. Comput., 28 (2006): 102-122.

[3] Blanco, P.J., Discacciati, M. and Quarteroni, A., Modeling dimensionally-heterogeneous problems: analysis, approximation and applications, Numer. Math., 119 (2011): 299-335.

[4] Blanco, P.J., Trenhago, P.R., Fernandes, L.G. and Feijóo, R.A., On the integration of the baroflex control mechanism in a heterogeneous model of the cardiovascular system. Int. J. Numer. Methods Biomed. Eng., 28 (2012): 412-433.

[5] Blanco, P.J., Urquiza, S.A. and Feijóo, R.A., Assessing the influence of heart rate in local hemodynamics through coupled 3D-1D-0D models. Int. J. Numer. Methods in Biomed. Eng., 26 (2010): 890-903.

[6] Boyer, F., Hubert, F., Krell, S., Non-overlapping Schwarz algorithm for solving 2D m-DDFV schemes, IMA J. Numer. Anal., 30 (2010); 1062-1100.

[7] Cai, X.-C. and Sarkis, M., A restricted additive Schwarz preconditioner for general sparse linear systems, SIAM J. Sci. Comput., 21 (1999): 792-797.

[8] Cautrés, R., Herbin, R. and Hubert, F., The Lions domain decomposition algorithm on non matching cell-centred finite volume meshes, IMA J. Numer. Anal., 24 (2004): 465-490.

[9] Chaouqui, F., Gander, M.J., Kumbhar, P.M., Vanzan, T., Linear and nonlinear substructured restricted additive Schwarz iterations and preconditioning, Numer. Algorithms, 91 (2022): 81-107.

[10] Ciaramella, G., Gander, M.J. , Iterative methods and preconditioners for systems of linear equations, SIAM (2022).

[11] Ciaramella, G., Vanzan, T. , Spectral Coarse Spaces for the Substructured Parallel Schwarz Method, J. Sci. Comput., 91 (2022): 69.

[12] Ciaramella, G., Vanzan, T. , Substructured two-grid and multi-grid domain decomposition methods, Numer. Algorithms, 91(2022): 413-448.

[13] Collino, F., Delbue, G., Joly, P. and Piacentini, A., A new interface condition in the non-overlapping domain decomposition for the Maxwell equations Helmholtz equation and related optimal control, Comput. Methods Appl. Mech. Engrg., 148(1997): 195-207.

[14] Deng, Q., An analysis for a nonoverlapping domain decomposition iterative procedure, SIAM J. Sci. Comput., 18 (1997): 1517-1525.

[15] Dimola, N., Kuchta, M., Mardal, K.-A., and Zunino, P., Robust Preconditioning of mixed-dimensional PDEs on 3d-1d domains coupled with Lagrange multipliers, Quantitative approaches to microcirculation: mathematical models, computational methods, measurements and data analysis (SEMA/SIMAI Collection on Microcirculation), 2024, Springer.

[16] Dolean, V., Gerardo-Giorda, L. and Gander, M.J., Optimized Schwarz methods for Maxwell equations, SIAM J. Sci. Comput., 31(2009): 2193-2213.

[17] Dolean, V., Jolivet, P. and Nataf, F., An introduction to domain decomposition methods: algorithms, theory and parallel implementation, SIAM, 2015.

[18] Engquist, B. and Majda, A., Absorbing boundary conditions for the numerical simulation of waves, Math. Comp., 31(1977): 629-651.

[19] Engquist, B. and Zhao, H.-K., Absorbing boundary conditions for domain decomposition, Appl. Numer. Math., 27(1998): 341-365.

[20] Gander, M.J., Optimized Schwarz methods, SIAM J. Numer. Anal., 44(2006): 699-731.

[21] Gander, M.J., Schwarz methods over the course of time, Electron. Trans. Numer. Anal., 31(2008): 228-255.

[22] Gander, M.J., Japhet, C., Maday, Y. and Nataf, F., A new cement to glue nonconforming grids with Robin interface conditions : the finite element case, Domain Decomposition Methods in Science and Engineering. Lecture Notes in Computer Science, Berlin, Springer, vol. 40 (2005): 259-366.

[23] Gander, M.J., Magoulès, F. and Nataf, F., Optimized Schwarz methods without overlap for the Helmholtz equation, SIAM J. Sci. Comput., 21(2002): 38-60.

[24] Gander, M.J. and Stuart, A.M., Space-time continuous analysis of waveform relaxation for the heat equation, SIAM J. Sci. Comput., 19 (1998): 2014-2031.

[25] Hagstrom, T., Tewarson, R. P. and Jazcilevich, A., Numerical Experiments on a Domain Decomposition Algorithm for Nonlinear Elliptic Boundary Value Problems, Appl. Math. Lett., 3(1988): 299-302.

[26] Halpern, L., Absorbing boundary conditions for the discretization schemes of the one-dimensional wave equation, Math. Comp., 38(1982): 415-429.

[27] Japhet, C. and Nataf, F., The best interface conditions for domain decomposition methods : absorbing boundary conditions, Artificial boundary conditions, with Applications to Computational Fluid Dynamics Problems, L. Tourette eds, 2000.

[28] Leiva, J.S., Blanco, P.J. and Buscaglia, G.S., Iterative strong coupling of dimensionally heterogeneous models, Internat. J. Numer. Methods Engrg., 81 (2010): 1558-1580.

[29] Leiva, J.S., Blanco, P.J. and Buscaglia, G.S., Partitioned analysis for dimensionally-heterogeneous hydraulic networks, SIAM Multiscale Model. Simulat., 9 (2011): 872-903.

[30] Lesinigo, M., D'Angelo, C. and Quarteroni, A., A multiscale Darcy-Brinkman model for fluid flow in fractured porous media, Numer. Math., 117 (2011):717-752.

[31] Lions, P. L., On the Schwarz algorithm method III : a variant for nonoverlapping subdomains, Third international Symposium on Domain Decomposition Methods for Partial Differential Equations, T.F. Chan, R. Glowinski, J. Periaux and O.B. Widlung eds, SIAM Philadelphia, PA, (1990): 202-223.

[32] Nataf, F. and Rogier, F., Factorisation of the Convection-Diffusion Operator and the Schwarz Algorithm Math. Models Methods Appl. Sci., 5(1995): 67-93.

[33] Panasenko, G.P., Method of asymptotic partial decomposition of domain, Math. Models Methods Appl. Sci., 8(1998): 139-156.

[34] Panasenko, G.P. and Viallon, M.-C., Error estimate in a finite volume approximation of the partial asymptotic domain decomposition, Math. Meth. Appl. Sci. 36(2013): 1892-1917.

[35] Panasenko, G. and Viallon, M.-C., Finite volume implementation of the method of asymptotic partial domain decomposition for the heat equation on a thin structure, Russian J. Math. Phys., 22 (2015): 237-263.

[36] Panasenko, G. and Viallon, M.-C., Method of asymptotic partial decomposition with discontinuous junctions, Comput. Math. Appl., 105 (2022): 75-93.

[37] Quarteroni, A. and Formaggia, L., Mathematical Modelling and Numerical Simulation of the Cardiovascular System, Modelling of Living Systems, Handbook of Numerical Analysis Series. N. Ayache editor, 2002.

[38] Quarteroni, A. and Valli, A., Domain Decomposition Methods for Partial Differential Equations, Oxford Science Publications, 1999.

[39] Rawat, V. and Lee, J.-F., Nonoverlapping domain decomposition with second order transmission condition for the time-harmonic Maxwell's equations, SIAM J. Scient. Comput., 32(2010): 3584-3603.

[40] Saad, Y., Iterative Methods for Sparse Linear Systems, SIAM, 2003.

[41] Viallon, M.-C., Domain decomposition methods in a geometrical multi-scale domain using finite volume schemes, Internat. J. Numeri. Methods Fluids, 92(2020): 391-421.

[42] Viallon, M.-C., Error estimate for a finite volume scheme in a geometrical multi-scale domain, M2AN, 49(2015): 529-550.

Université Jean Monnet Saint-Étienne, CNRS, Institut Camille Jordan UMR 5208, F-42023, Saint-Étienne, France

E-mail: `canon@univ-st-etienne.fr`

URL: `http://www.ucs.lousiana.edu/~hxy6615/`